Interim Report | *Covering the Period 5 April to 31 August 1967*

INVESTIGATIONS OF LASER DAMAGE TO OCULAR TISSUES

By: A. VASSILIADIS - N. PEPPERS - K. DEDRICK - H. CHANG - R. C. HONEY
H. C. ZWENG, M. D. - R. R. PEABODY, M. D. - H. ROSE, M. D. - M. FLOCKS, M. D.

Prepared for:

AIR FORCE AVIONICS LABORATORY
SYSTEMS ENGINEERING GROUP
RESEARCH AND TECHNOLOGY DIVISION
UNITED STATES AIR FORCE
WRIGHT-PATTERSON AIR FORCE BASE, OHIO

CONTRACT F33615-67-C-1752

STANFORD RESEARCH INSTITUTE
MENLO PARK, CALIFORNIA

STANFORD RESEARCH INSTITUTE
MENLO PARK, CALIFORNIA

September 1967

Interim Report | *Covering the Period 5 April to 31 August 1967*

INVESTIGATIONS OF LASER DAMAGE TO OCULAR TISSUES

Prepared for:

AIR FORCE AVIONICS LABORATORY
SYSTEMS ENGINEERING GROUP
RESEARCH AND TECHNOLOGY DIVISION
UNITED STATES AIR FORCE
WRIGHT-PATTERSON AIR FORCE BASE, OHIO

CONTRACT F33615-67-C-1752

By: A. VASSILIADIS - N. PEPPERS - K. DEDRICK - H. CHANG - R. C. HONEY
H. C. ZWENG, M. D. - R. R. PEABODY, M. D. - H. ROSE, M. D. - M. FLOCKS, M. D.

SRI Project 6680

Approved: D. R. SCHEUCH, EXECUTIVE DIRECTOR
ELECTRONICS AND RADIO SCIENCES

ABSTRACT

Preliminary results of experimental investigations of minimally sized retinal lesions caused by neodymium lasers are presented. The experimental animals were rhesus monkeys. Data for both long-pulse neodymium and Q-switched neodymium lasers are included.

Results of experimental investigation for threshold damage by a CW CO_2 laser to rabbit corneas are also presented. Data for two exposure times are included. In addition, theoretical calculations based on a one-dimensional heat-flow model are reported, and comparison is made with the experimental results.

CONTENTS

ILLUSTRATIONS

I INTRODUCTION

This report presents the progress on a program to study the effects of laser radiation on ocular tissue. The overall objectives of the program are to determine the threshold levels for damage to ocular tissue using a variety of lasers. This report is a summary of work in progress, and accordingly, some of the results presented herein are preliminary.

The development of the laser has aroused considerable interest in the study of laser damage to ocular tissues both for safety considerations and for possible clinical applications to eye disorders. The work under this program concerns the determination of thresholds for damage to ocular tissues. The investigations are carried out under conditions that simulate the accidental exposure most likely to occur during field use. Thus, for lasers in the visible and near-infrared regions, retinal damage thresholds are determined for conditions of minimum retinal spot size. For the case of longer wavelength infrared radiation, specifically corneal damage caused by the CO_2 laser, exposure times shorter than the blink reflex are investigated for exposure areas of at least several square millimeters.

In previous investigations,[1,2*] threshold measurements for ruby-lasers operated in the long-pulse, Q-switched, and mode-locked modes of operation were reported. Also preliminary investigations of CO_2 corneal damage were reported.[2] In the present program, more significant data have been and will be obtained for CO_2 corneal damage at different exposures and for Q-switched operation. Theoretical calculations have also been made for corneal damage using a thermal interaction and relaxation model. In addition, retinal damage data are to be obtained for neodymium long-pulse, Q-switched, and mode-locked modes of operation. Finally, more data will be obtained for the Q-switched and mode-locked ruby lasers.

---

*References are listed at the end of the report.

In this interim report, preliminary data are presented for neodymium-laser retinal damage. Both long-pulse and Q-switched neodymium laser data are included. Experimental data for CO_2 laser damage for two exposure times are presented along with extensive theoretical calculations for the thermal damage to the cornea.

II EXPERIMENTS ON RETINAL DAMAGE

A. Experimental Configuration and Procedures

The experimental test station is shown schematically in Fig. 1. It is constructed around a Zeiss fundus camera, which provides the means of monitoring the retina of the experimental animals during the experiments. As shown in the diagram, the laser beam is introduced

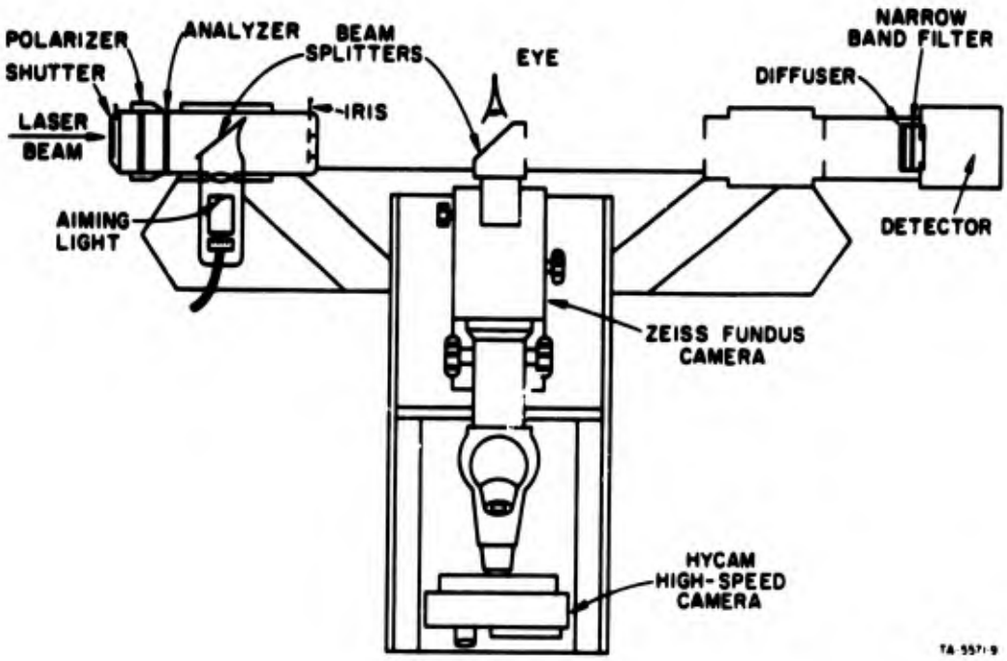

FIG. 1 DIAGRAM OF EXPERIMENTAL TEST STATION

from the left. The first element is a shutter, whose operation controls the experiment. That is, after the shutter has been triggered open by the ophthalmologist, the oscilloscope shutters are opened, after which the laser is fired. Thus, with the entrance shutter closed, misfires of the laser cannot result in accidental exposure to personnel or animals at the test station. The laser beam then propagates through a polarizer/analyzer combination, which permits variable attenuation of the laser beam. After the polarizer/analyzer, a collimated white light

beam, which is coaxial with the laser beam path, is introduced by the use of a beam splitter. The light beam provides a means of aiming the laser beam; the spot created by this light on the retina coincides with the location of the laser beam. The final component in this part of the station is a limiting iris, which can be varied to permit adjustment of the beam diameter to the required cross-section to ensure that the entire beam passes through the pupil of the eye during a retinal exposure.

Upon leaving the limiting iris, the beam strikes a dichroic beam splitter, which is mounted on the Zeiss fundus camera. The beam splitter is located and oriented such that the aiming light, the laser beam, and the illumination light source of the fundus camera are coaxial as they enter the experimental animal's eye. The dichroic beam splitter diverts the majority of the laser beam into the animal's eye, and the remainder of the laser beam continues on to the monitoring equipment. This consists of a diffuser, a narrow-band filter, attenuators, and a calibrated high-speed detector. A photograph of the terminal test station is shown in Fig. 2, where the various elements can be clearly seen. Although a 16-mm high-speed camera is shown in the camera position, conventional 35-mm color photographs are usually taken with the standard Zeiss camera back during most experiments.

Ideally, any laser beam that is used in these experiments should be of uniform intensity in its cross section and very well collimated. These ideal conditions are not fulfilled by the beams from present-day pulsed solid-state lasers; accordingly, the experimental configurations must be designed to satisfy these requirements as well as possible.

Some desirable conditions may be produced by propagating the laser beam over an appreciable distance before introducing it into the experimental test station. This long path length serves two functions. First, the inherent hot-spots in the original laser beam become comparable to, or larger than, the pupil of the eye as the beam diverges; thus, a relatively uniform intensity beam is obtained over an area defined by the iris diaphragm. Second, because of the small size of the laser aperture

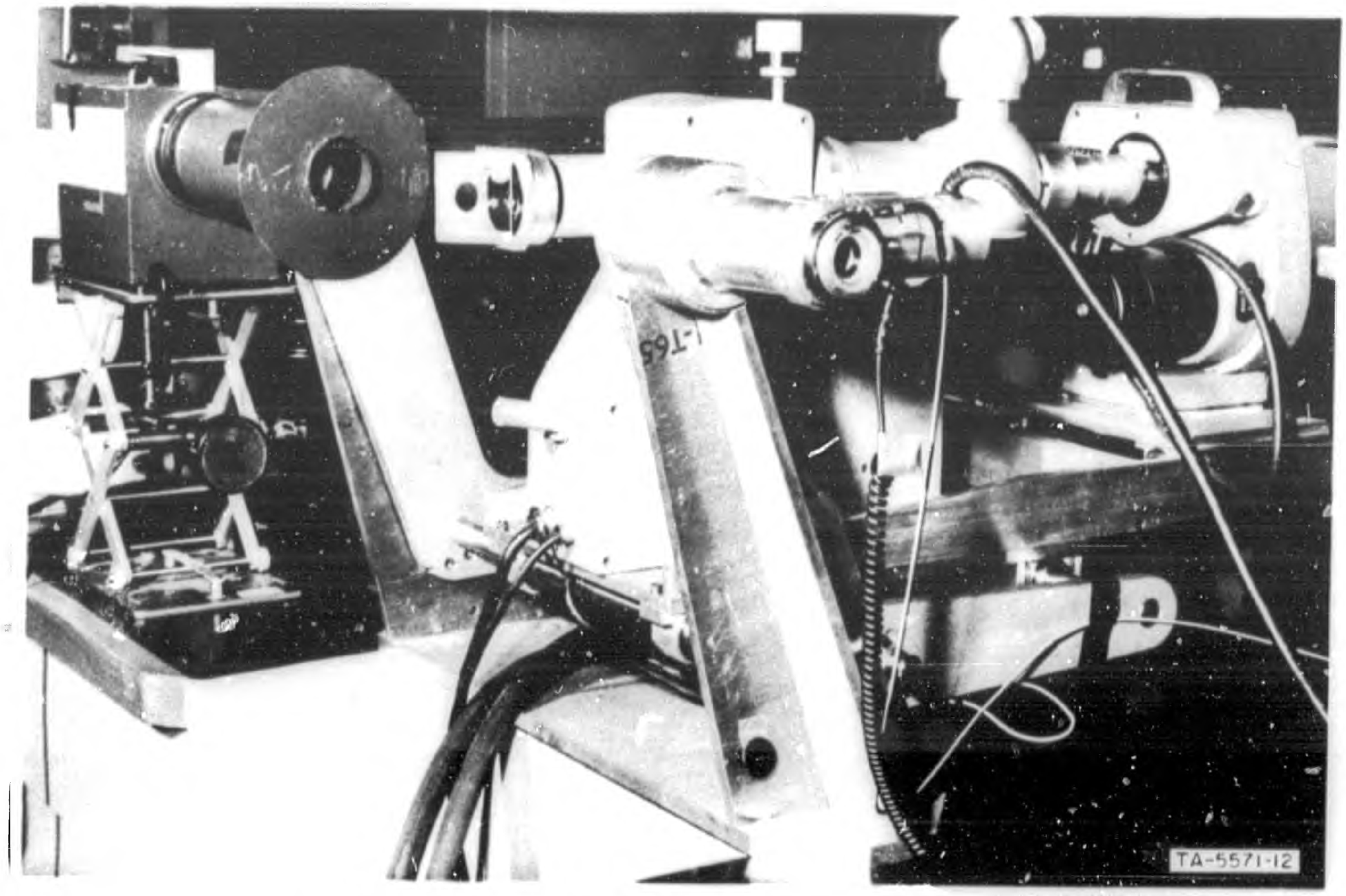

FIG. 2 PHOTOGRAPH OF EXPERIMENTAL TEST STATION

and the pupil of the eye and the large distance from the laser to the eye, only the eye optics will limit the minimum size of the retinal impact area.

The laser is easily and accurately aligned with the experimental test station, a routine procedure at the beginning of an experiment, by the use of a He-Ne CW laser. Calibration is accomplished by placing a thermopile at the locus of the animal's eye and measuring the energy at the thermopile and at the detector that is used as the monitor. Frequent cross checking among several available energy measuring devices insures reliable and consistent data.

The procedures employed in the preparation of a monkey have been reported previously.[1,2] Cycloplegia is assured by the use of one percent atropine, and the animal is tranquilized and anesthetized. The eyes are

then refracted and the required corrective lens is inserted in front of the eye to obtain minimum retinal spot sizes.

B. Neodymium Laser Experiments

1. Laser Characteristics

The laser makes use of a 6-inch glass rod with Brewster angle cuts. The rod is pumped by two 12-mm-bore linear flash lamps in a close-coupled configuration. The lamps have arc lengths of 6.5 inches and are air cooled while the glass laser rod is water cooled. The resonant cavity consists of a homosil quartz roof prism on one end and a sapphire flat Fabry-Perot etalon at the output end. A photograph of the laser cavity is shown in Fig. 3. The laser can be operated either in the long-pulse or Q-switched mode. Q-switching is achieved by the use of a

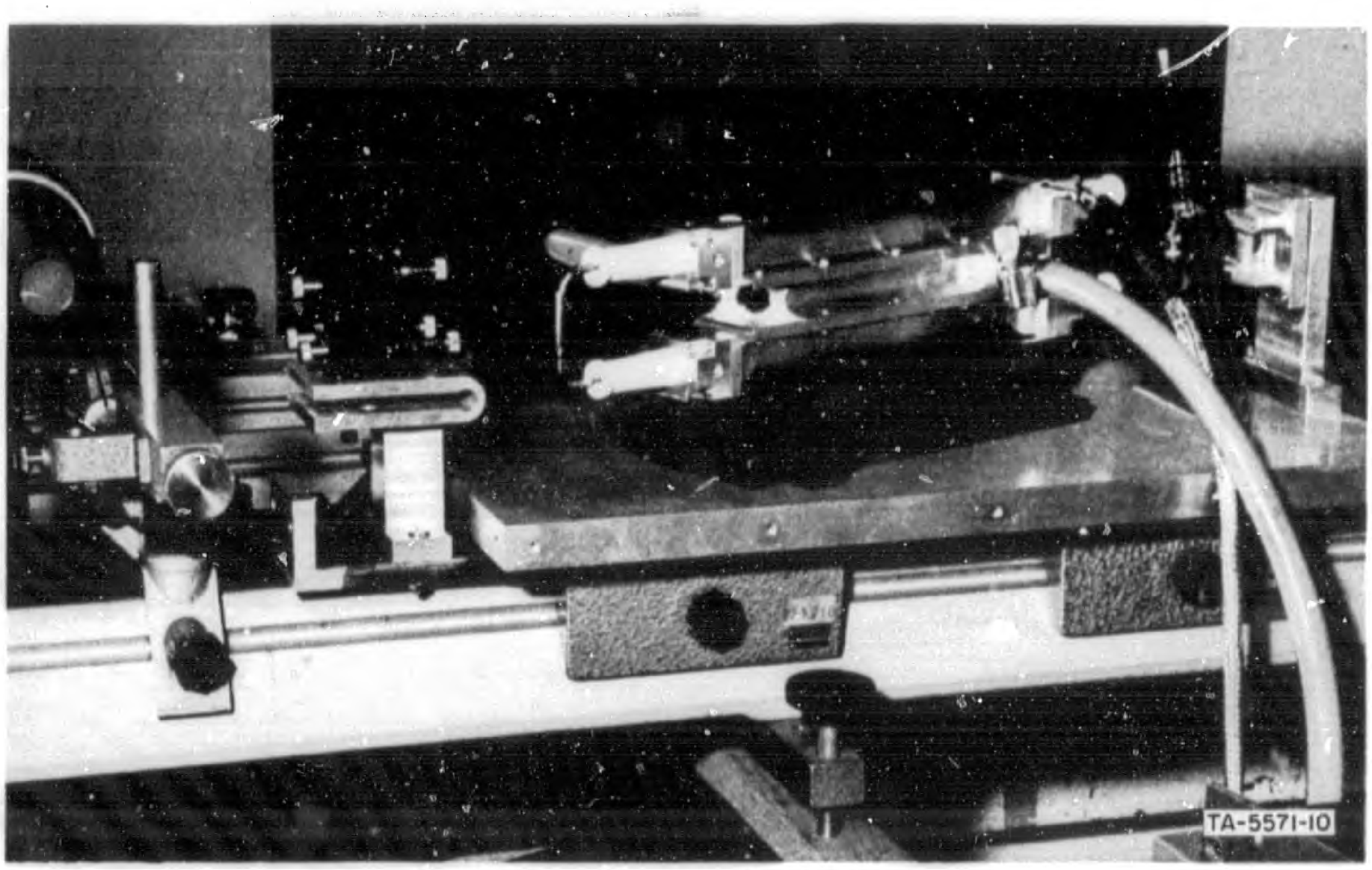

FIG. 3 PHOTOGRAPH OF NEODYMIUM LASER CAVITY

saturable dye placed in a fused quartz cuvette between the glass rod and the roof prism. The dye that has been used in the experiments is

Kodak dye EK-9740 diluted with chloro-benzene so that a transmission of approximately 55 percent is obtained at 1.06μ. This dye deteriorates upon exposure to light; however, even though the cuvette is not shielded from flash-lamp light, several tens of shots can be obtained before appreciable cell deterioration is noticed.

In the long-pulse mode of operation, the pulse train that was used in the experiments is shown in Fig. 4. This trace is the output of a photodiode that shows the pump light and the laser output train. The laser burst is approximately 600 μs in duration.

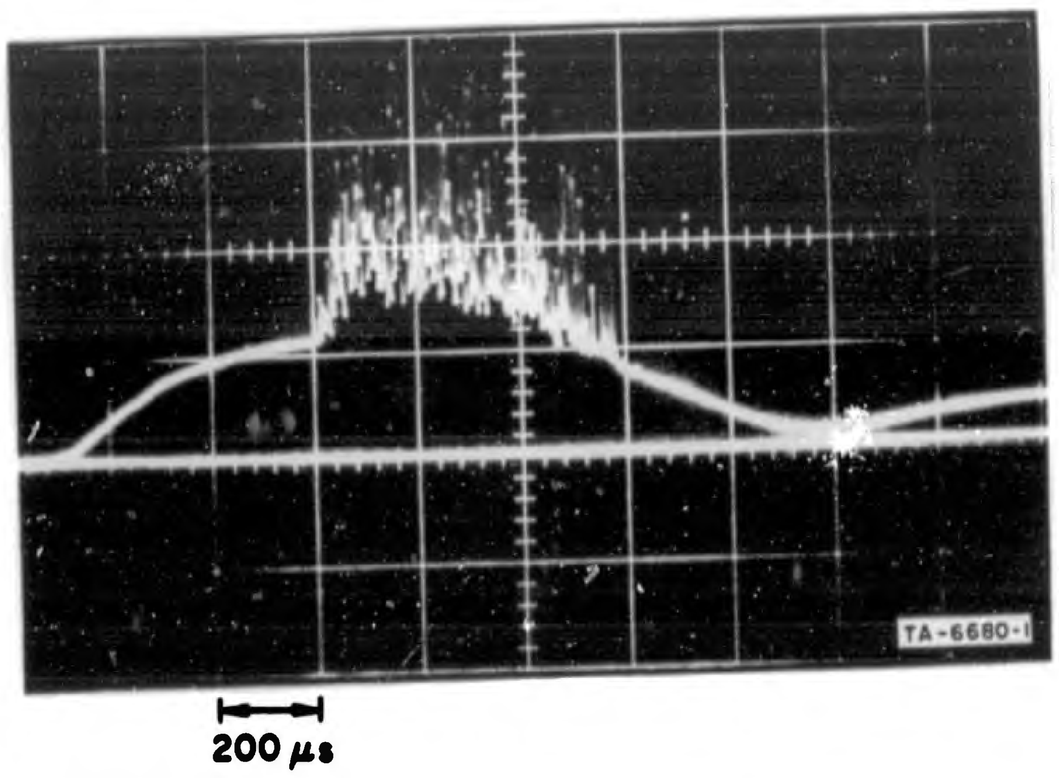

FIG. 4 TRACE SHOWING PUMP LIGHT AND LASER PULSE-TRAIN

In the Q-switched mode of operation, the output of the monitor diode shows a single giant pulse. A biplanar photodiode, in conjunction with a Tektronix 519 oscilloscope, shows the pulse to be approximately 30 ns in duration. A typical trace of a Q-switched pulse is shown in Fig. 5.

2. Long-Pulse Experiments

Rhesus monkeys are employed in all experiments for retinal threshold determination. The preliminary data that is presented here has been obtained on peripheral regions of rhesus monkey retinas, i.e.,

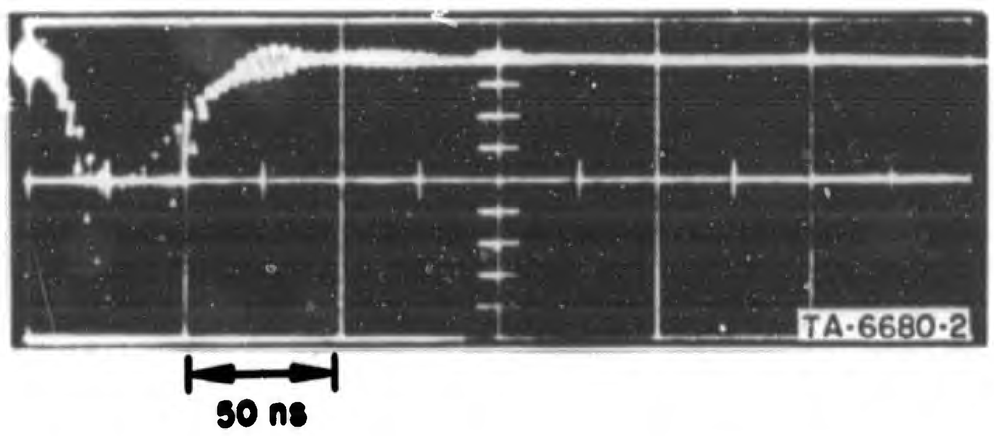

FIG. 5 TRACE SHOWING TYPICAL Q-SWITCHED PULSE

in the region around the macula but not on the macula. Macular data will be obtained in the future along with additional paramacular data.

The data was gathered using the experimental configuration described in the previous section. A photograph of the experimental arrangement is shown in Fig. 6. At the beginning of an experiment a Polaroid photograph is taken of the retina and is subsequently used as a map. During and after the experiment, 35-mm color photographs are taken periodically. The monkey's retina is under constant observation, through the Zeiss fundus camera and all exposure sites are recorded on a Polaroid photograph. These sites are observed for at least one hour after exposure. A lesion is noted as observed at an exposure site if an ophthalmoscopically visible response appears within one hour after exposure.

In the long-pulse experiments performed to date with the neodymium laser, characteristic responses similar to those observed with the ruby long-pulse laser were noted. Thus, at near threshold levels, no immediate response is observed at the site of impact; however, a small white patch interpreted as edema is seen to develop within a few minutes or longer, depending on the level. At somewhat higher

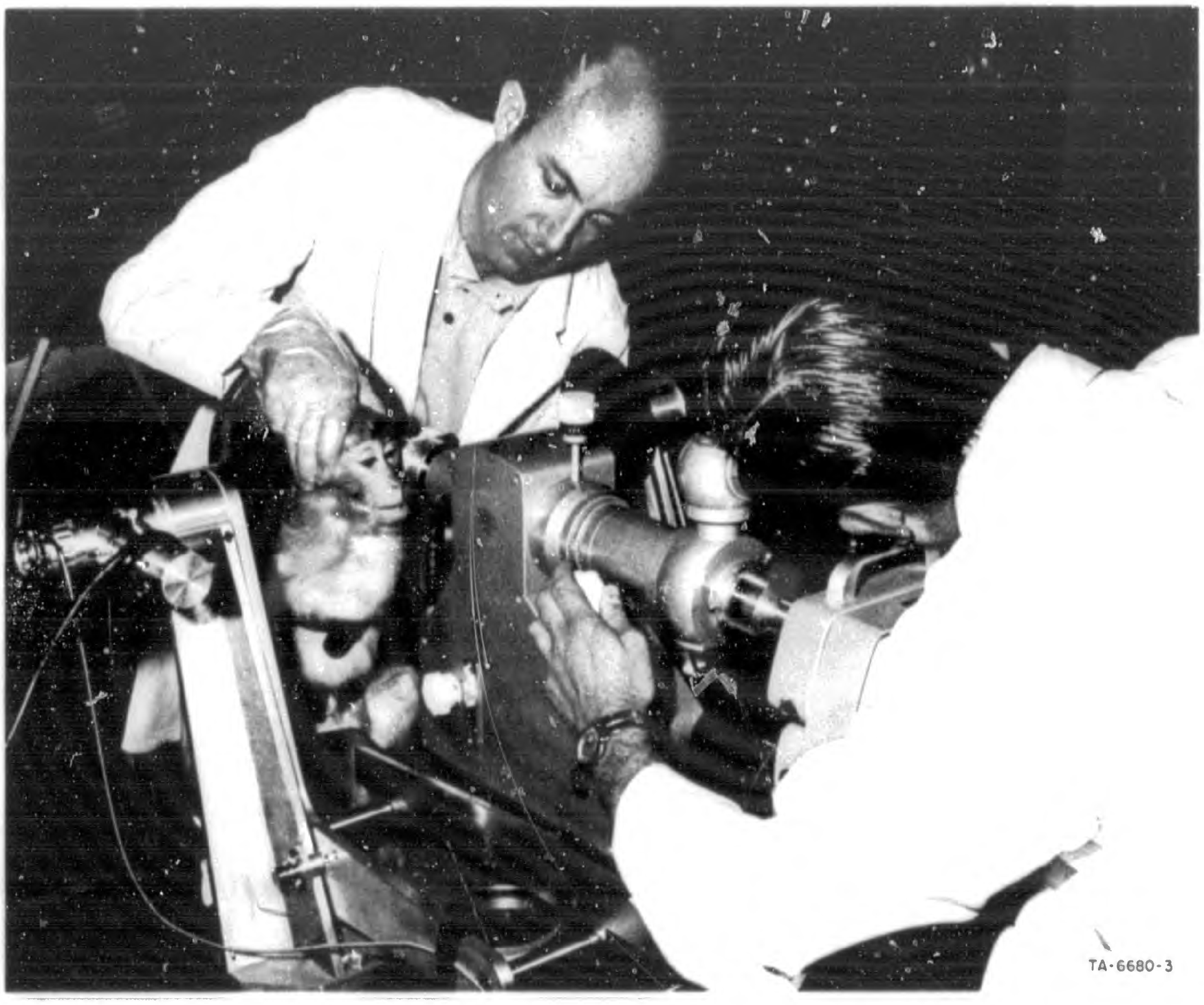

FIG. 6 PHOTOGRAPH OF TEST STATION DURING EXPERIMENT

energy values however, an immediate response is observed, which is interpreted as a vapor bubble. This bubble quickly disappears and after several minutes a small white patch is seen to develop and grow somewhat in size. The appearance of the vapor bubble appeared at levels much closer to threshold than those observed in the ruby long-pulse exposures.

The data for the long-pulse neodymium is shown in Fig. 7, where the individual exposures are classified according to whether or not a lesion was observed, and are plotted as a function of total energy into the eye. The energy scale is then divided into equal logarithmic

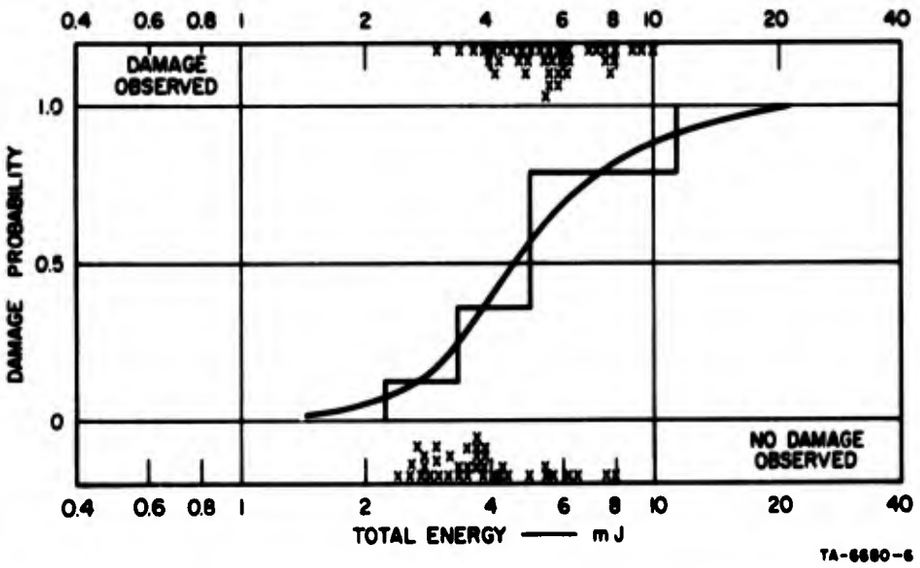

FIG. 7 LONG PULSE NEODYMIUM LASER DAMAGE ON RHESUS MONKEY RETINA

intervals, and a probability for damage is calculated for each interval, i.e., the number of exposures that caused detectable lesions divided by the total number of exposures within the interval. The histogram is then obtained and a smooth curve is drawn approximately through the histogram indicating the probability curve that might be obtained for a sufficiently large sample. From Fig. 7, it is apparent that the level that gives a 50 percent probability for damage is approximately 4.5 mJ of long-pulse neodymium energy into the eye.

Although a direct comparison cannot be made at this time because of the difference in pulse length used in the ruby long-pulse experiments[2] (1.7 ms) it appears that the neodymium long-pulse threshold (0.6 ms) is approximately four times higher than the ruby long-pulse data.

3. Q-Switched Experiments

The data for the Q-switched neodymium laser were obtained using the same experimental configuration and procedures. The laser was Q-switched, and, as noted in Sec. II, Part A-1, the pulse length was approximately 30 ns.

The retinal responses for these exposures are similar to those observed with the Q-switched ruby laser.[2] Thus, near threshold no response is seen for an appreciable time after exposure, depending on the level of the dose. As the level is increased, a point is reached where an immediate response is seen. This response is a small white patch interpreted as edema and is easily visible through the ophthalmoscope. Vapor bubbles are not observed up to the levels that have thus far been used and included in the following data.

The Q-switched data is summarized in Fig. 8, in a manner similar to that used for the long-pulse data. In this case, it is noted that the total energy required for a 50-percent probability for damage is approximately 150 μJ. A comparison with ruby Q-switched data is not directly possible since the ruby data was obtained for 8-ns pulses. Nevertheless, the ratio between the two cases shows the neodymium threshold is approximately six times the ruby threshold.

More data will be obtained for the Q-switched mode in the near future. In addition, the laser will be converted to mode-locked operation and threshold data will be obtained for these extremely short pulses.

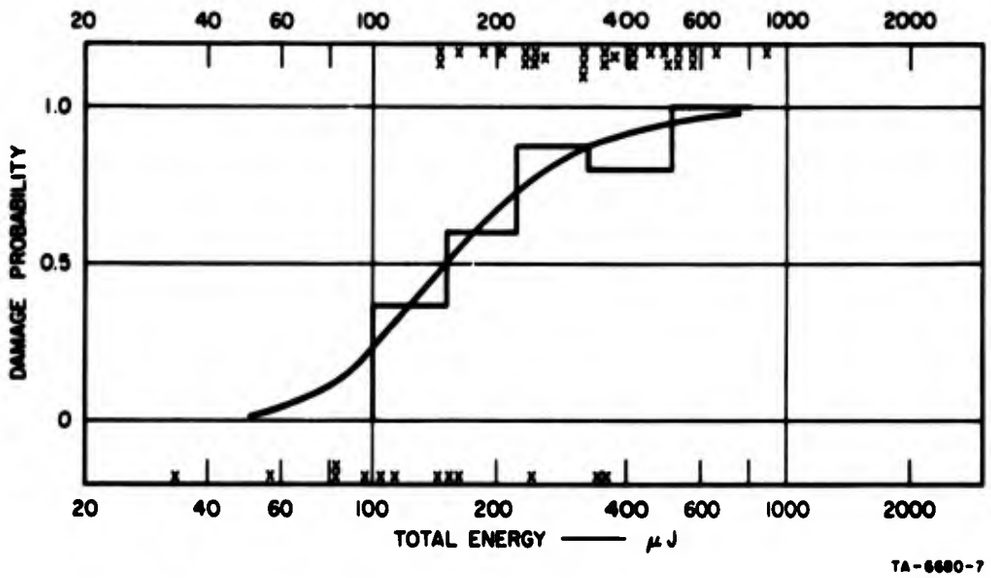

FIG. 8 Q-SWITCHED NEODYMIUM LASER DAMAGE ON RHESUS MONKEY RETINA

III EXPERIMENTS ON CORNEAL DAMAGE FROM CO_2 LASERS

A. Experimental Configuration and Procedures

The basic CO_2 laser configuration is similar to that described in a previous report.[2] However, by restricting the laser to single-mode operation the experimental procedure has been considerably simplified and the accuracy of the data has been substantially increased.

The laser cavity is two meters in length and makes use of a flat metal reflector at one end and a semi-transparent spherical mirror, which also serves as a lens, at the other end. The spherical mirror is made of dielectric coated germanium with curvatures such that the output of the laser is brought to a focus approximately 68 cm from the output mirror.

By placing an iris of appropriate size inside the resonant cavity, the higher-order transverse modes are discriminated against, and the laser is constrained to emit in the lowest-order transverse mode (TEM_{00}), for which the output beam intensity varies as a Gaussian distribution in its cross section. Such a Gaussian beam has the unique property that it retains its Gaussian distribution as it propagates. Thus, at any location away from the laser, although the beam comes to a focus and then diverges, its cross section is always a Gaussian distribution.

The size and distribution of the laser beam as a function of the distance from the laser was calculated from the known characteristics of the resonant cavity and output lens. The beam was also experimentally scanned at several locations using a thermopile with a small aperture. Figure 9 shows the excellent agreement between the theoretically calculated Gaussian curve for one of the locations where the beam was experimentally scanned. The agreement between theory and experiment also gives a good indication of the temporal stability of the laser since the double scan that represents the experimental points required approximately 13 minutes to complete.

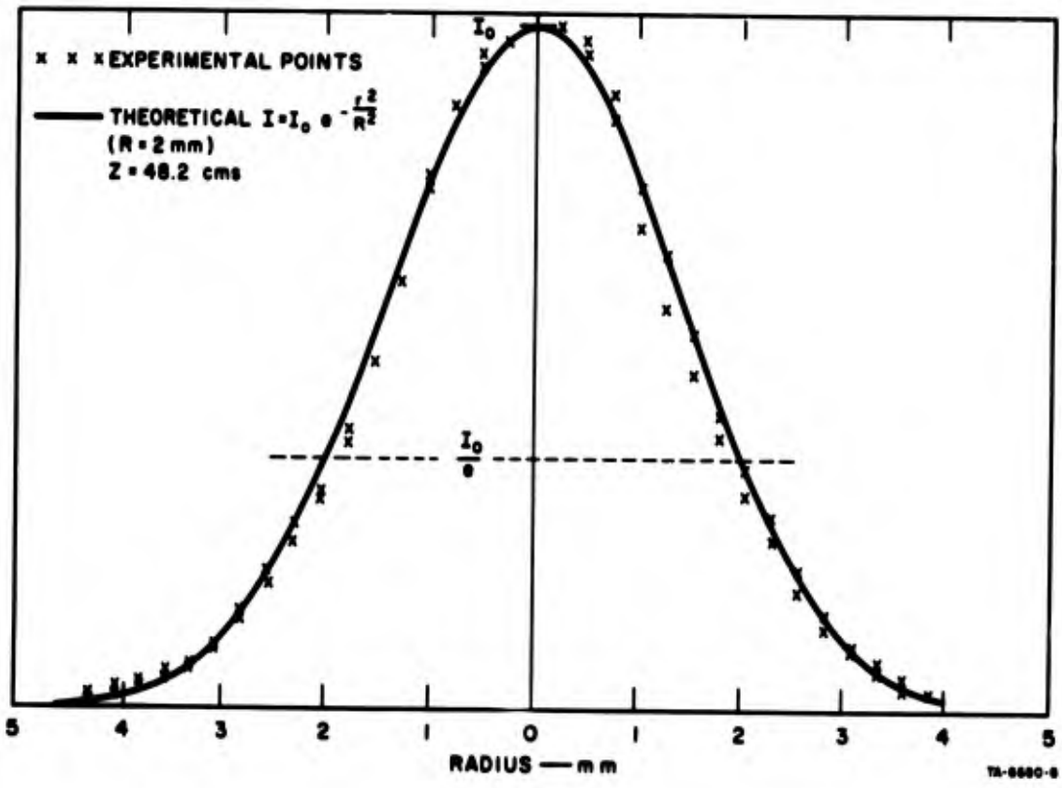

FIG. 9 DISTRIBUTION OF CO_2 LASER BEAM

The excellent agreement between the theory and the experimental observations made it possible to establish the width of the beam for experimental exposures by simply noting the distance of the target surface from the laser output or from the focus. With regard to the beamwidth or spot size of the exposure, it has been decided to use the distance between 1/e values of the beam as the width rather than the distance between 1/2 power values. The reason for this is that the (1/e) value for beamwidth gives the nice feature that the average value of intensity assuming all the energy in the beam is within the 1/e beamwidth coincides with the peak value of intensity of the Gaussian distribution.

The experimental configuration is illustrated in Fig. 10. The laser beam is blocked by an asbestos sheet while the experimental animal's eye is properly located and positioned with the aid of a low power He-Ne laser beam that is introduced coaxially with the CO_2 beam

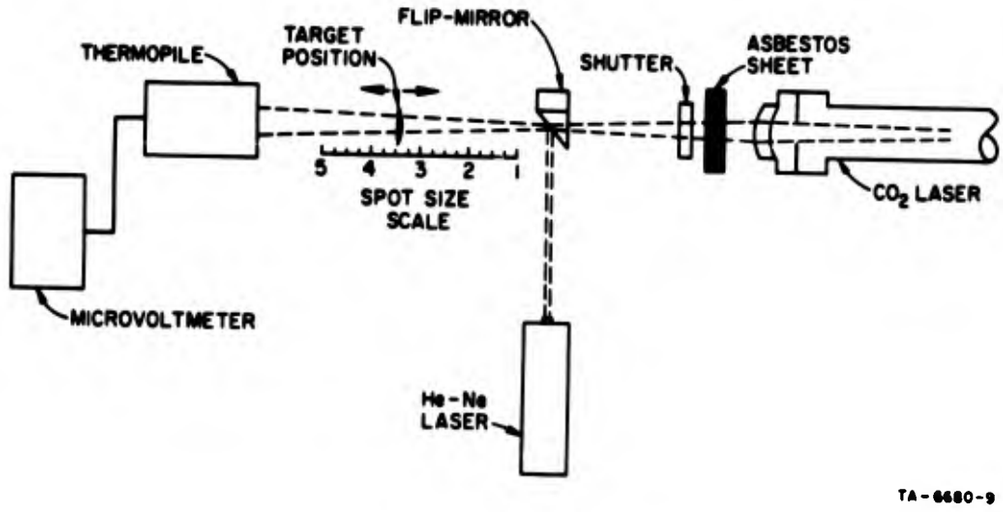

FIG. 10 DIAGRAM OF CO_2 LASER EXPERIMENTAL CONFIGURATION

path by a flip mirror. The eye is positioned carefully for the selected spot size by use of a calibrated scale that has been calculated as outlined above. Small variations in power density and spot size may be easily obtained by varying the distance. With the animal in position, the flip mirror is spun out of the way, and the shutter is triggered after the asbestos sheet has been removed. The animal is then pulled back out of the path of the beam and an identical shuttered exposure is placed into the ballistic thermopile. Since the laser stability with time has been shown to be excellent, this sequential reading of the energy in the exposure is satisfactory since the repeatability of the calibrated shutter has been tested and shown to be very good. This system was also calibrated by the use of an Eppley thermopile that was exposed to a fraction of the laser beam. Comparison of the power output measured by the two methods showed agreement to better than three percent.

B. Experimental Measurement of Corneal Damage

Radiation from the CO_2 laser at 10.6μ presents a hazard to the eye because this radiation is highly absorbed in the cornea of the eye.

In order to assess the damage to the ocular tissues, experimental animals are being used to establish damage thresholds to the cornea.

Since normal sensitivity to pain at the cornea makes exposures longer than the blink reflex unlikely, only exposures under 100 ms are being examined in this experimental program.

An accidental exposure would involve an appreciable fraction of the cornea; thus, experimental exposures should cover an appreciable area. Theoretically, the diameter of the exposed area in the experiments must be large compared to the depth of absorption in the tissue. Since the absorption coefficient of the cornea is estimated as approximately 1000 cm^{-1}, an exposure diameter of 2 to 3 mm would be more than adequate for the determination of threshold levels for the cornea.

The measurements on corneal damage were made on rabbit corneas using the experimental configuration and procedures outlined in the previous section. Figure 11 is a photograph of the laser and the experimental arrangement. Each eye received usually three, but not more than five, exposures and was then carefully examined through a Zeiss binocular photo slit lamp as shown in Fig. 12.

An exposure was defined as a lesion if a corneal opacity was seen at the impact location within ten minutes after the exposure. At the threshold level, a minimal opacity is observed in the corneal epithelium. Under slit lamp examination, the opacity appears as a white surface haze that shows no elevation or swelling. This change is attributed to the denaturization of proteins due to the temporary temperature changes of the surface of the cornea. A photograph of such a minimal lesion is shown in Fig. 13. At higher levels, the opacity is more pronounced and dense, the lesion begins swelling, and after a few minutes epithelial cells are sluffed off from parts of the lesions and small cratering is observed. An example at about twice threshold is shown in Fig. 14. All the lesions that are discussed below, which go up to levels approximately three times threshold, healed completely without visible scarring within 24 to 48 hours after exposure.

Although more exposure times are planned, only two sets of data are included in this report. The first set of data was taken at an exposure time of 55 ms. The data are presented in Fig. 15 as damage probability

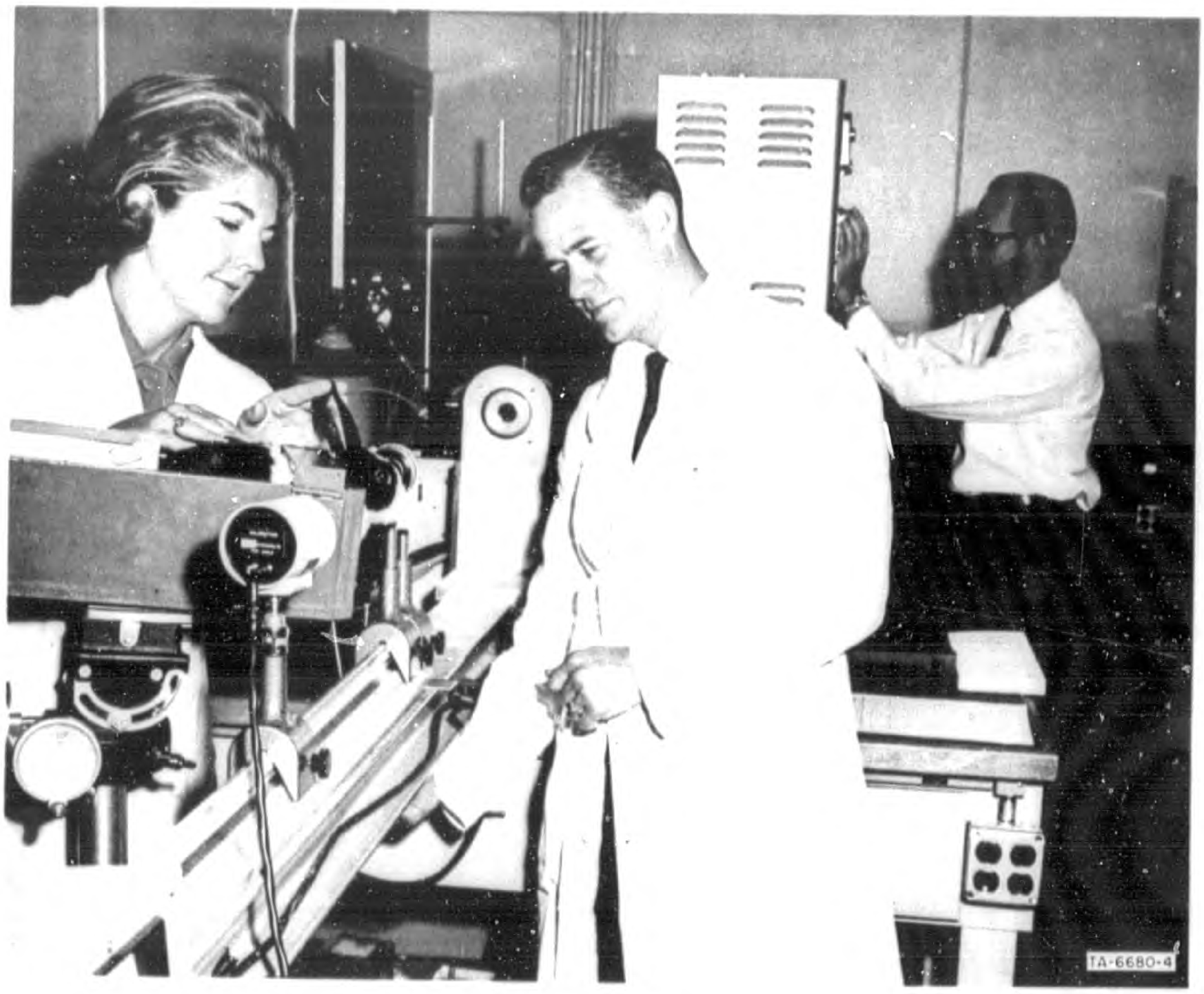

FIG. 11 PHOTOGRAPH OF CO_2 LASER EXPERIMENTAL ARRANGEMENT

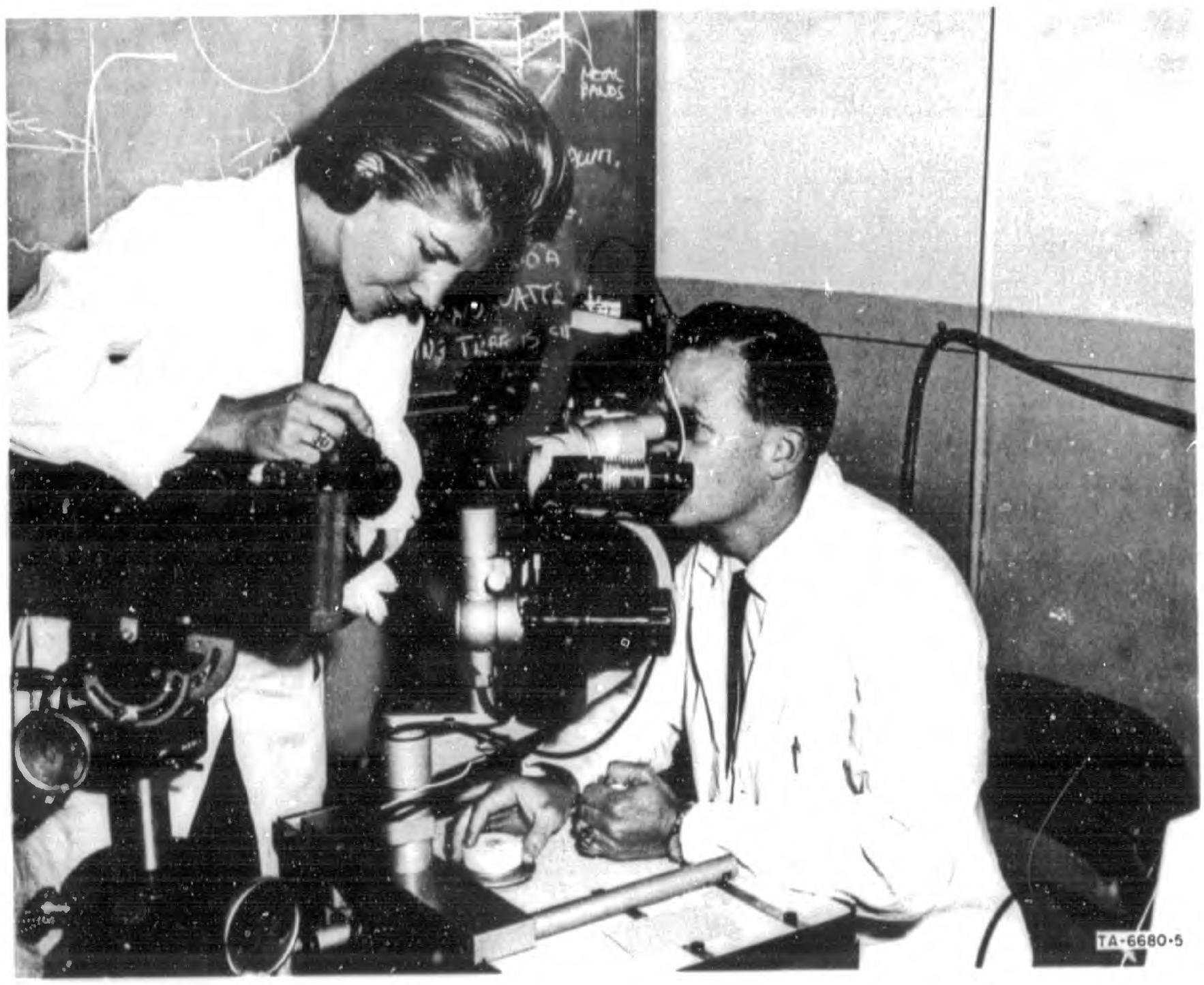

FIG. 12 PHOTOGRAPH SHOWING PHOTO-SLIT LAMP IN USE

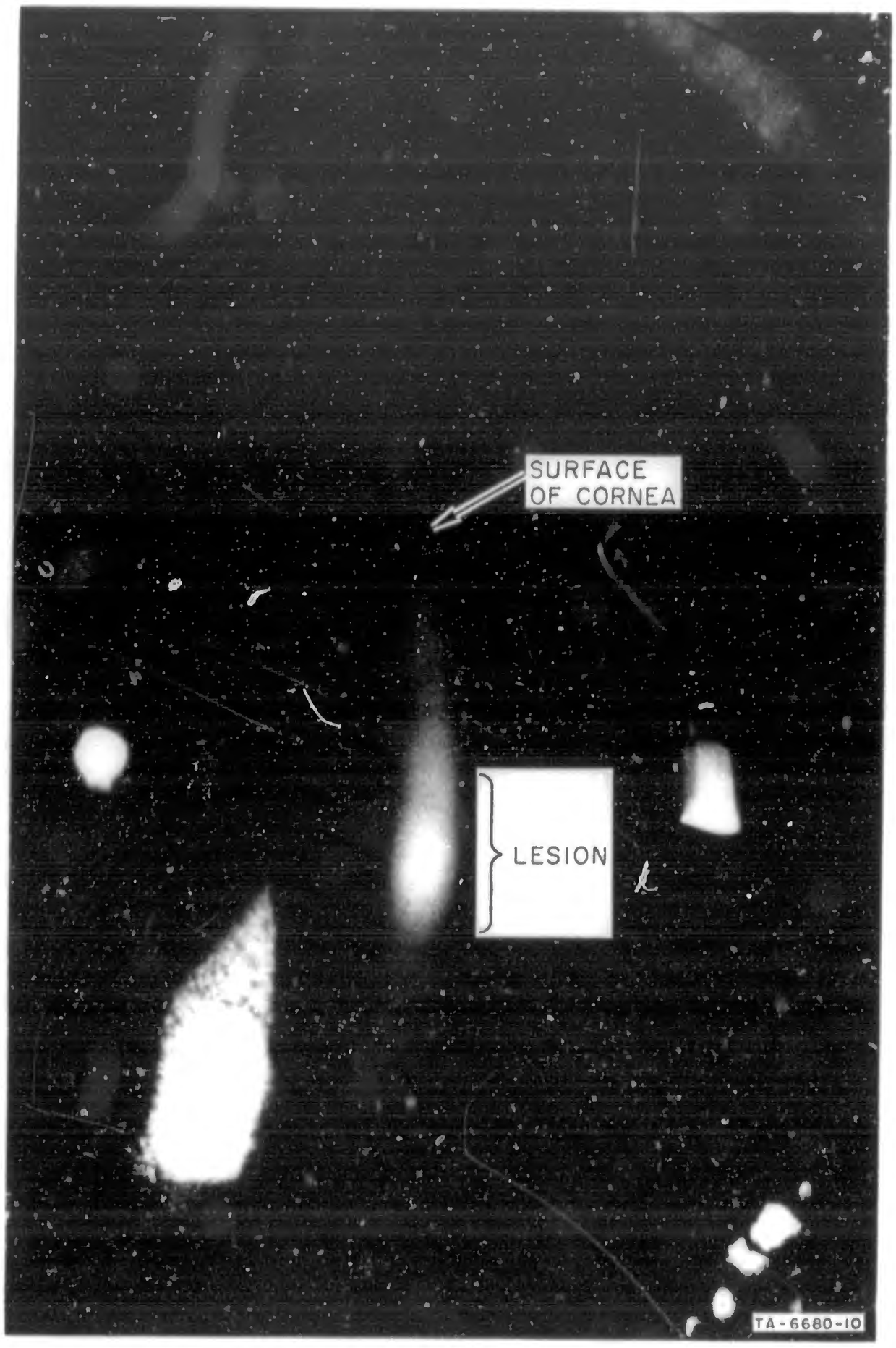

FIG. 13 PHOTOGRAPH OF MINIMAL LESION SEEN THROUGH SLIT LAMP

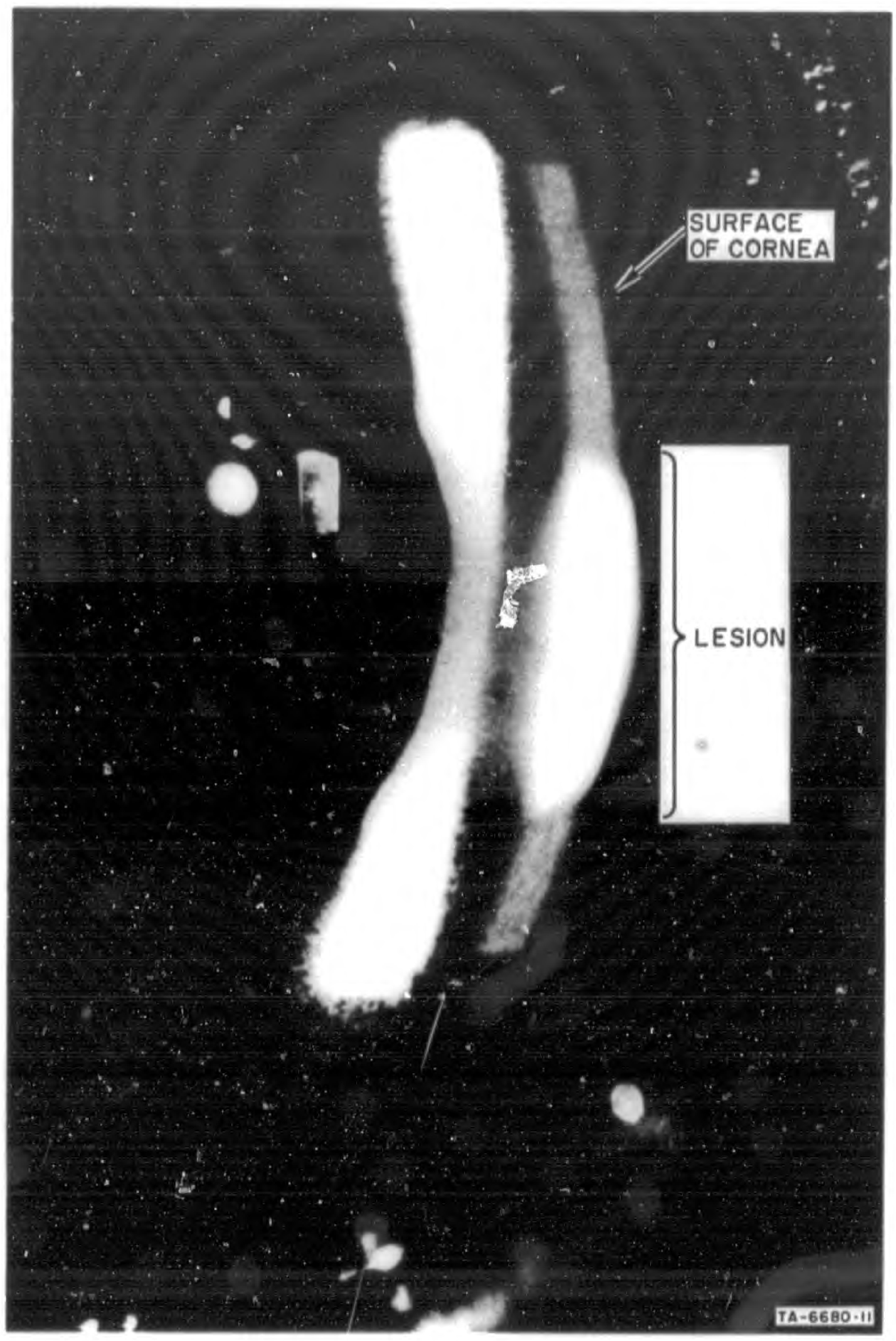

FIG. 14 PHOTOGRAPH OF LESION AT TWICE-THRESHOLD LEVEL

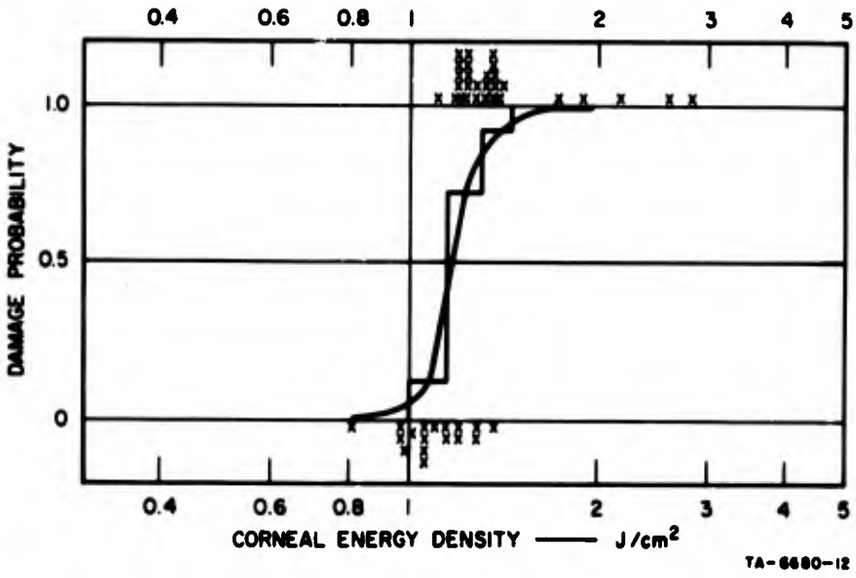

FIG. 15 CO_2 CORNEAL DAMAGE FOR 55-ms EXPOSURE

as a function of energy density. From the figure, it is apparent that 1.2 J/cm^2 is required for the threshold of damage. This corresponds to a power density of approximately 22 W/cm^2. The sharp transition from no damage to damage reflects the accuracy of the experimental procedures, and the critical temperature dependence of protein denaturation.

Additional data were taken for 10 ms exposure times. The results for this exposure are summarized in Fig. 16. From the figure, it is seen that the threshold for damage for this exposure is 0.77 J/cm^2. This corresponds to a power density of 77 W/cm^2.

A comparison of threshold energy densities for the two exposure times shows that at the shorter exposure damage was observed at a lower level. Since the denaturation of proteins should take place at about the same temperature for the two exposures, the difference is due presumably to the thermal conduction into the deeper layers of the cornea.

The interaction of the 10.6μ radiation of the CO_2 laser and the cornea can be theoretically treated using a simple model that is physically meaningful. For this reason, it was decided to carry out some theoretical calculations in order to determine the temperature rise associated with the threshold lesions. These calculations could be

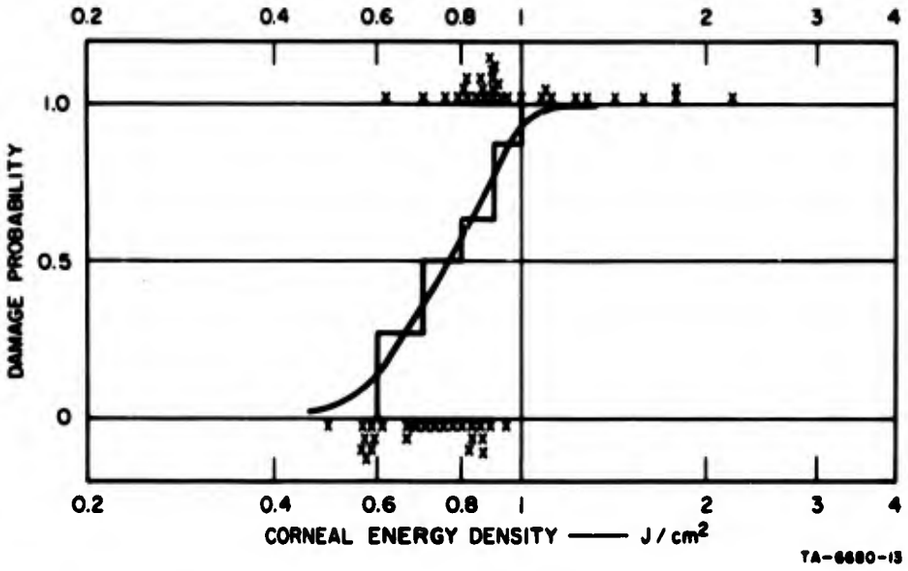

FIG. 16 CO_2 CORNEAL DAMAGE FOR 10-ms EXPOSURE

used to develop means for confidently extrapolating the experimental data to other exposure times.

C. Theoretical Study of Corneal Damage

The heating of the cornea by CO_2 laser radiation is studied using a simple one-dimensional model.

The incident laser beam is assumed to be uniform and incident normally on an infinite plane interface representing the cornea. The heat flow is thus one dimensional and flows into the cornea. It is assumed that reradiation from the surface is negligible and that the cornea has thermal properties close to those of water, and that they do not change with temperature. The model further assumes that there is no steam formation; thus temperatures above 100°C cannot be treated with this model. This is not a limitation for threshold damage analysis since protein denaturation takes place at temperatures appreciably below the boiling point of water. The incident radiation is assumed to be a square pulse in time.

The one-dimensional heat-flow equation may be written in the form:

$$\frac{\partial \psi}{\partial t} = a^2 \frac{\partial^2 \psi}{\partial x^2} + a^2 u_o e^{-\gamma x} \tag{1}$$

for $x \geq 0$, where

$$u_o = \frac{\gamma S_o}{4.18 \kappa}$$

ψ = temperature (°C)

γ = absorption coefficient (cm^{-1})

S_o = incident power density (W/cm^2)

κ = heat conductivity ($cal\text{-}cm/cm^2 - s°C$)

$a^2 = \kappa/\rho c$ = diffusivity (cm^2/s)

ρ = density (g/cm^2)

c = heat capacity ($cal/g - °C$)

t = time (s)

x = depth (cm).

The incident power density, S_o, is first taken to be a Heaviside step function at $t = 0$. Then the solution to Eq. (1), when S_o is a step function, may be obtained by various methods. A simple method of solution is outlined in the Appendix where the solution is shown to be:

$$\psi(x,t) = \frac{u_o}{\gamma}\left\{2\gamma\left(\frac{a^2 t}{\pi}\right)^{1/2} e^{-\frac{x^2}{4a^2 t}} - e^{-\gamma x} - \gamma x \operatorname{erfc}\left(\frac{x}{2\sqrt{a^2 t}}\right) + \frac{1}{2} e^{\gamma^2 a^2 t}\left[e^{\gamma x} \operatorname{erfc}\left(\gamma\sqrt{a^2 t} + \frac{x}{2\sqrt{a^2 t}}\right) + e^{-\gamma x} \operatorname{erfc}\left(\gamma\sqrt{a^2 t} - \frac{x}{2\sqrt{a^2 t}}\right)\right]\right\}, \tag{2}$$

which agrees with the solution of Carslaw and Jaeger.[3]

Since a square pulse of duration τ can be written as the difference of two Heaviside functions, the solution of Eq. (1) when S_o is a square pulse, can be written in terms of Eq. (2) by using the principle of superposition. That is,

$$\psi_p(x,t) = U(t)\,\psi(x,t) - U(t-\tau)\,\psi(x,\,t-\tau) \quad , \qquad (3)$$

where $U(\xi)$ is the Heaviside unit step function.

Computer calculations were made for Eq. (2) using dimensionless variables defined by:

$$X = \frac{\gamma x}{2}$$

$$\tau = \gamma a \sqrt{t} \quad . \qquad (4)$$

$$\Psi = \gamma^2 \frac{\psi}{u_o}$$

Parametric calculations for these variables were obtained on a computer, and some of the results are plotted in Fig. 17 where the normalized temperature, Ψ, is plotted versus normalized time of exposure, τ, for various normalized depths, X. From this figure it is possible to calculate temperature rise and decay at any depth for different values of the parameters of the medium and different levels of incident radiation. A comparison of theoretical calculations and experimental data is made in the next section.

D. Comparison of Theoretical and Experimental Results

In this preliminary comparison between theory and experiment, it will be assumed that the cornea has the properties of water and that they do not change with temperature. Thus, we assume:

$\gamma = 1030\ (cm^{-1})$

$\kappa = 0.00144\ [cal\ cm/(cm^2\ s^\circ C)]$

$\rho = 1.00\ (g/cm^3)$

$c = 1.00\ [cal/(g^\circ C)]$.

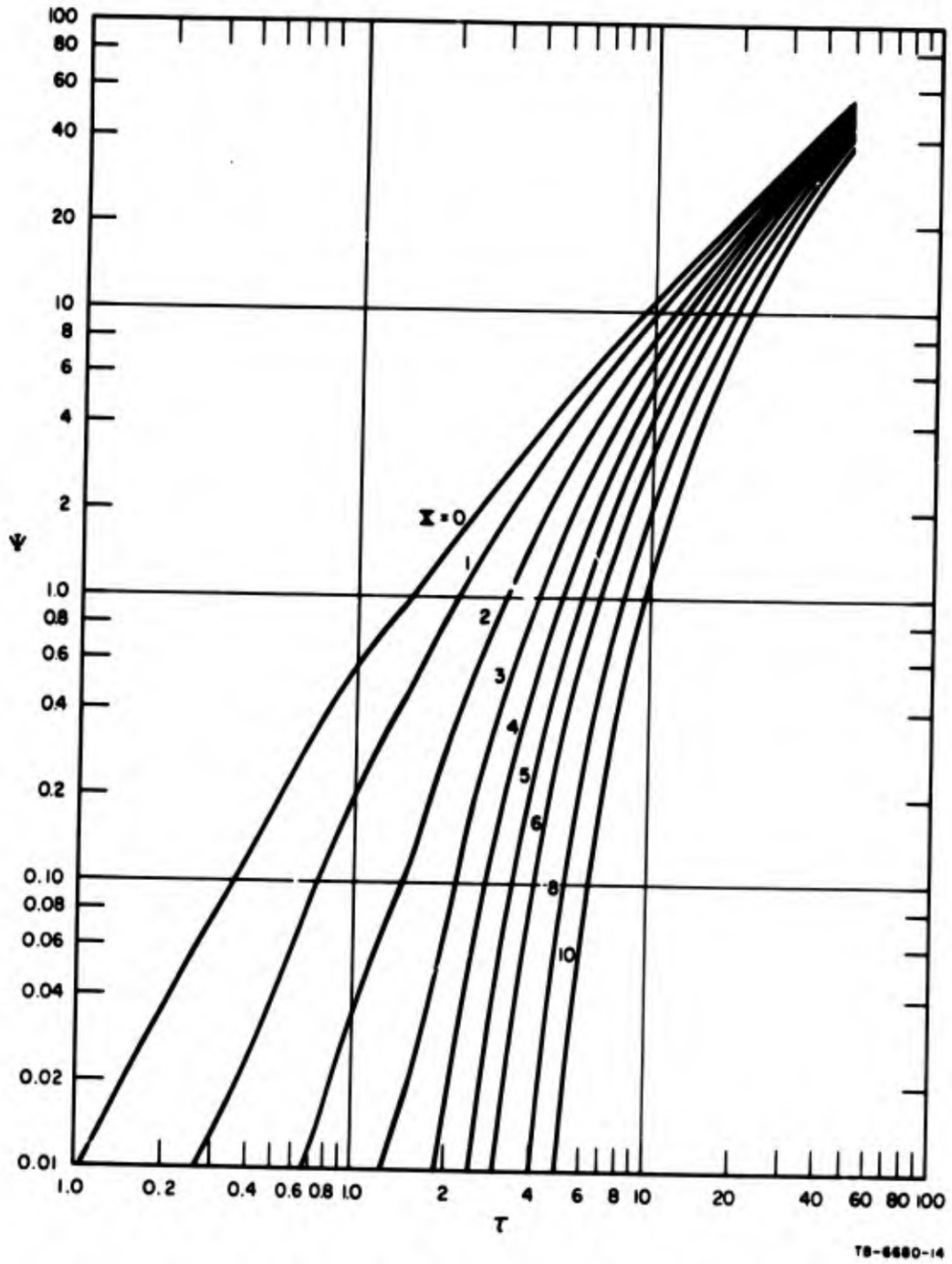

FIG. 17 THEORETICAL CALCULATIONS FOR TEMPERATURE VARIATIONS

Using these values we find, using Eq. (4)

$$X = 515\ x$$

$$\tau = 39.1\sqrt{t} \quad . \tag{5}$$

$$\Psi = \frac{6.2\ \psi}{S_o}$$

Thus, using these relations and recalling Eq. (3), the temperature profile at various depths may be obtained for any pulse width with the aid of Fig. 17.

For a comparison with the experimental measurements, the maximum temperature change that occurs at the surface of the cornea for a given exposure is calculated. The relations shown in Eq. 5 are used with $x = 0$, and the incident power density required to cause a given temperature change is determined from Fig. 17 for various pulse lengths. A series of these constant-temperature curves is plotted in Fig. 18.

Entered in the same graph are the experimental points obtained from measurements on rabbit corneas. For the 55 ms exposure, a temperature rise of about 32°C is indicated while, for the 10 ms exposure, a temperature rise of about 44°C is obtained.

The temperature rise at the surface, when calculated for both experimental cases, is somewhat higher than would be expected for the denaturation of protein. There are two reasons why the experimental results will tend to be high. First, since the beam that is used has a Gaussian form, and because the lesion size observed at threshold, although smaller than the beam size (1/e value), still has appreciable physical extent, the value of the energy density that causes the damage at the edge of the lesion is lower than the quoted value that corresponds to the peak value. Thus, one way to obtain more accuracy in this matter may be to measure the size of the lesion observed for each exposure and relate it to the actual value of energy density at the edge of the lesion using the known Gaussian distribution. Second, the surface

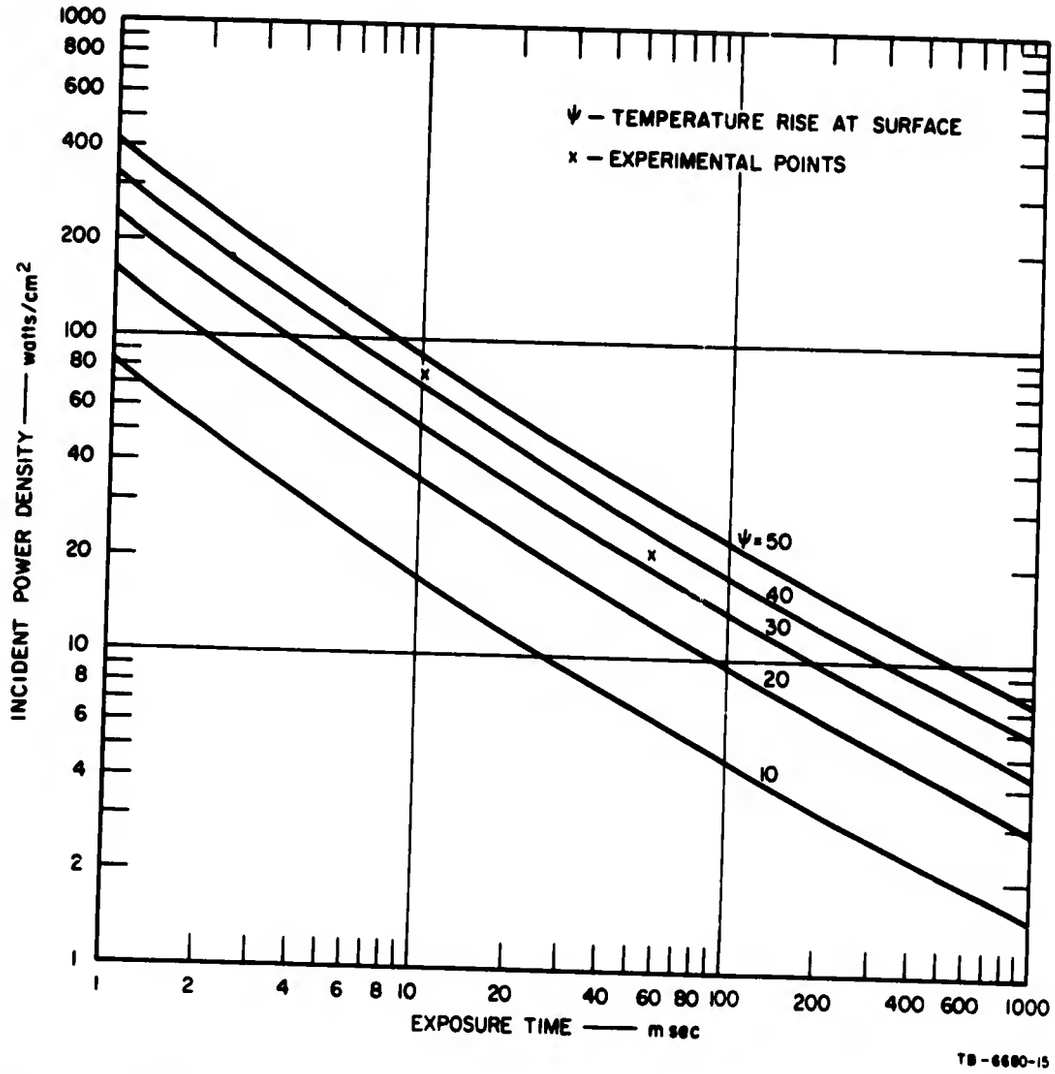

FIG. 18 COMPARISON OF THEORY AND EXPERIMENTAL DATA OF CORNEAL DAMAGE

of the layer of tears that is present in the eye, since it also has properties similar to water, will act as the surface of interaction. Thus, if the tear layer is 10μ thick, then the surface of the cornea would be at $x = 10\mu$ ($X = 0.515$) and thus (see Fig. 17) the cornea will not reach as high a temperature as the surface of the tears ($x = 0$).

The difference between the values of temperature calculated for the two exposures is partly explained by the presence of the tear layer. Since the tear layer will act as the interacting surface, the temperature reached by the cornea will be proportionally lower at the shorter

exposures as evidenced by the spreading apart of the curves in Fig. 17 at the lower values of τ. Another possible explanation for the difference in temperature may be that it is an indication that the proteins can withstand higher temperatures during shorter exposures before denaturation takes place. However, additional measurements at shorter exposures are required before a conclusion can be reached in this regard.

IV CONCLUSIONS

The experiments on retinal damage using neodymium lasers ($\lambda = 1.06\mu$) and minimum retinal spot sizes are still in progress. The preliminary data presented in this report show that for long-pulse neodymium (pulse length of 0.6 ms) an energy of 4.5 mJ is required to 50-percent probability of damage on the monkey retina. For Q-switched neodymium, for a 30-ns pulse, an energy of 150 μJ is required for 50-percent probability of damage.

With regard to CO_2 laser ($\lambda = 10.6\mu$) corneal damage, data for two exposure times are reported. For a pulse of 55 ms, the corneal energy density for threshold damage is 1.2 J/cm^2 corresponding to 22 W/cm^2 power density. For a pulse length of 10 ms, the damage threshold energy density is 0.77 J/cm^2 corresponding to 77 W/cm^2 power density. Theoretical calculations for thermal damage using a one-dimensional model are presented and compared to this experimental data. They show good agreement although the calculated temperature rises are somewhat higher than expected.

APPENDIX

SOLUTION OF THE ONE-DIMENSIONAL HEAT-FLOW PROBLEM

In this appendix, a summary of a simple method of solution of the one-dimensional heat-flow problem is presented.

The heat-flow equation:

$$\frac{\partial^2 \psi(x,t)}{\partial x^2} - \frac{1}{a^2} \frac{\partial \psi(x,t)}{\partial t} = - u_o \, e^{-\gamma x} \qquad \text{(A-1)}$$

is to be solved subject to the following boundary conditions

$$\psi(x,o) = 0$$

$$\left.\frac{\partial \psi(x,t)}{\partial x}\right]_{x=0} = 0 \qquad \text{i.e., no heat flow at } x = 0 \text{ boundary.}$$

where the conductive medium fills the half space $x \geq 0$ and $x < 0$ is vacuum.

A solution is easily obtained by the use of the Green's function. The Green's function $G(x - x', t - t')$ satisfies the equation

$$\frac{\partial^2 G}{\partial x^2} - \frac{1}{a^2} \frac{\partial G}{\partial t} = - \delta(x - x') \, \delta(t - t') \qquad \text{(A-2)}$$

and must satisfy the following boundary conditions:

$$G(x - x', t - t') = 0 \quad \text{when} \quad \tau = t - t' < 0$$

and

$$\left.\frac{\partial G}{\partial x}\right]_{x=0} = 0 \quad .$$

It is easily verified[4] that

$$G(x - x', \tau) = \frac{a}{2\sqrt{\pi\tau}} \left[e^{-\frac{(x-x')^2}{4a^2\tau}} + e^{-\frac{(x+x')^2}{4a^2\tau}} \right] U(\tau) \qquad \text{(A-3)}$$

where $U(\tau)$ is the Heaviside unit step function.

It follows[4] that

$$\psi(x,t) = \frac{au_o}{2\sqrt{\pi}} \int_o^t \frac{dt'}{\sqrt{\tau}} \int_o^\infty e^{-\gamma x'} \left[e^{-\frac{(x-x')^2}{4a^2\tau}} + e^{-\frac{(x+x')^2}{4a^2\tau}} \right] dx' \quad . \qquad \text{(A-4)}$$

The integrals in Eq. (A-4) can be easily carried out, and the solution is found to be

$$\psi(x,t) = \frac{u_o}{\gamma^2} \left\{ 2\gamma a \sqrt{\frac{t}{\pi}}\, e^{-\frac{x^2}{4a^2t}} - e^{-\gamma x} - \gamma x \operatorname{erfc}\left(\frac{x}{2a\sqrt{t}}\right) \right.$$

$$\left. + \frac{1}{2} e^{\gamma^2 a^2 t} \left[e^{\gamma x} \operatorname{erfc}\left(\gamma a\sqrt{t} + \frac{x}{2a\sqrt{t}}\right) + e^{-\gamma x} \operatorname{erfc}\left(\gamma a\sqrt{t} - \frac{x}{2a\sqrt{t}}\right) \right] \right\} \quad . \qquad \text{(A-5)}$$

ACKNOWLEDGMENTS

The authors acknowledge with gratitude the contributions of L. E. Alterton and E. J. Scribner for the design, construction, and operation of the experimental equipment and Miss A. Hammond for her assistance in the experiments.

REFERENCES

1. A. Vassiliadis, R. C. Rosan, R. R. Peabody, H. C. Zweng, R. C. Honey, "Investigation of Retinal Damage Using a Q-Switched Ruby Laser," Special Technical Report, SRI Project 5571, Contract AF 33(615)-3060, Stanford Research Institute, Menlo Park, California (August 1966).

2. A. Vassiliadis, N. A. Peppers, R. R. Peabody, R. C. Rosan, H. C. Zweng, M. Flocks, R. C. Honey, "Investigations of Laser Damage to Ocular Tissues," Technical Report AFAL-TR-67-120, SRI Project 5571, Contract AF 33(615)-3060, Stanford Research Institute, Menlo Park, California (March 1967).

3. H. Carslav, J. Jaeger, Conduction of Heat in Solids, (2nd ed.) p. 80 (Oxford, Clarendon Press, 1959).

4. P. M. Morse, H. Feshbach, Methods of Theoretical Physics, p. 857f (McGraw-Hill Book Co., Inc., New York, New York, 1953).

UNCLASSIFIED

Security Classification

DOCUMENT CONTROL DATA - R & D

(Security classification of title, body of abstract and indexing annotation must be entered when the overall report is classified)

1 ORIGINATING ACTIVITY (Corporate author)
Stanford Research Institute
333 Ravenswood Avenue
Menlo Park, California 94025

2a. REPORT SECURITY CLASSIFICATION
UNCLASSIFIED

2b. GROUP
N/A

3 REPORT TITLE

INVESTIGATIONS OF LASER DAMAGE TO OCULAR TISSUES

4 DESCRIPTIVE NOTES (Type of report and inclusive dates)
Interim Report 5 April to 31 August 1967

5 AUTHOR(S) (First name, middle initial, last name)
A. Vassiliadis - N. Peppers - K. Dedrick - H. Chang - R. C. Honey
H. C. Zweng, M.D. - R. R. Peabody, M.D. - H. Rose, M.D. - M. Flocks, M.D.

6. REPORT DATE
September 1967

7a. TOTAL NO. OF PAGES
39

7b. NO. OF REFS
4

8a. CONTRACT OR GRANT NO.
F33615-67-C-1752

b. PROJECT NO.

c.

d. Work unit: 5244.09 004

9a. ORIGINATOR'S REPORT NUMBER(S)
Interim Report
SRI Project 6680

9b. OTHER REPORT NO(S) (Any other numbers that may be assigned this report)

10. DISTRIBUTION STATEMENT
This document has been approved for public release and sale; its distribution is unlimited.

11. SUPPLEMENTARY NOTES

12. SPONSORING MILITARY ACTIVITY
Air Force Avionics Laboratory
Systems Engineering Group
Research and Technology Division, USAF
Wright-Patterson Air Force Base, Ohio

13 ABSTRACT

Preliminary results of experimental investigations of minimally sized retinal lesions caused by neodymium lasers are presented. The experimental animals were rhesus monkeys. Data for both long-pulse neodymium and Q-switched neodymium lasers are included.

Results of experimental investigation for threshold damage by a CW CO_2 laser to rabbit corneas are also presented. Data for two exposure times are included. In addition, theoretical calculations based on a one-dimensional heat-flow model are reported, and comparison is made with the experimental results.

DD FORM 1 NOV 68 1473 (PAGE 1)

S/N 0101-807-6801

UNCLASSIFIED

Security Classification

14 KEY WORDS	LINK A		LINK B		LINK C	
	ROLE	WT	ROLE	WT	ROLE	WT
Lasers						
Retinal Damage						
Corneal Damage						
Opthalmology						